On the Mechanism of Acetylcholinesterase Action: The Electrostatically Induced Acceleration of the Catalytic Acylation Step

Stanislaw T. Wlodek,*,† Jan Antosiewicz,‡ and James M. Briggs*,§

Contribution from the Texas Center for Advanced Molecular Computation, University of Houston, Houston, Texas 77204-5502, Department of Biophysics, University of Warsaw, Warsaw 02-089, Poland, and Department of Pharmacology, University of California, San Diego, La Jolla, California 92093-0365

Received February 5, 1997[⊗]

Abstract: Brownian dynamics simulations of the encounter kinetics between the active site of the wild-type and Glu199 mutant of Torpedo californica acetylcholinesterase (TcAChE) with a charged substrate were performed. In addition, ab initio quantum chemical calculations using the 3-21G basis set were undertaken to probe the energetics of the transformation of the Michaelis complex into a covalently bound tetrahedral intermediate using various models of the wild-type and Glu199Gln mutant active sites. The quantum calculations predicted about a factor of 32 reduction in the rate of formation of the tetrahedral intermediate upon the Glu199Gln mutation and showed that the Glu199 residue located in the proximity of the enzyme active triad boosts AChE's activity in a dual fashion: (1) by increasing the encounter rate due to the favorable modification of the electric field inside the enzyme reaction gorge and (2) by stabilization of the transition state for the first chemical step of catalysis. Our calculations also demonstrate the critical role of the oxyanion hole in stabilization of the tetrahedral intermediate and suggests that a charge relay mechanism may operate in the Glu199Gln mutant AChE as opposed to a general base mechanism as in the wild-type enzyme.

Introduction

Acetylcholinesterase (AChE) is one of the most efficient enzymes from the family of serine hydrolases, operating at a rate approaching the diffusional limit.[1−3] Solution of the crystal structure of Torpedo californica AChE (TcAChE),[4] showed that the enzyme contains a catalytic triad, Glu-His-Ser in a mirror image relationship to that present in other serine hydrolases in which the members of the triad are normally Asp-His-Ser.[5−7] This triad is, however, located at the bottom of a narrow, 20 Å deep gorge. The very high activity of AChE must then be the result of numerous interactions with a substrate acetylcholine (ACh^+). A number of experimental and modeling studies have already revealed several important factors contributing to the efficiency of AChE. In particular, modeling studies[8,9] and recent solution of the X-ray structure of a transition state analog complexed with TcAChE[10] revealed the existence of a three-pronged oxyanion hole formed by peptidic NH groups from Gly118, Gly119, and Ala201, in contrast to two-pronged oxyanion holes in serine proteases.[11−13] The results of Brownian dynamics simulations suggest that the electrostatic field of the enzyme contributes largely to the guidance of the positively charged substrate to the bottom of the active site gorge, supported, in part, by previous work[14] and that described in this paper. Finally, site-directed mutagenesis studies have indicated a crucial role of quaternary ammonium binding locus components: Trp84,[8] Phe330,[15] and Glu199.[16,17] The role of Glu199, whose carboxyl group is located in close proximity to the catalytic His440 residue, seems to be more complex than merely that of increasing the binding strength of the charged substrate, ACh^+. It has been suggested[18] that this residue provides a driving force for leading the ACh^+ substrate to the active site. In fact, the Glu199Gln mutation not only yields an enzyme with a several times increased K_m, as initially shown by Gibney et al.,[19] but also the value of k_{cat}/K_m is decreased even more dramatically: by 50-fold according to Radić et al.[16] and about 100-fold according to the most recent study of Quinn et al.[17] In both studies, the authors suggest that Glu199 provides a specific

* Corresponding authors.
† University of Houston.
‡ University of Warsaw.
§ University of California, San Diego.
⊗ Abstract published in *Advance ACS Abstracts,* August 15, 1997.

(1) Nolte, H. J.; Rosenberry, T. L.; Neumann, E. *Biochemistry* **1980**, *19*, 3705−3711.
(2) Hassinoff, B. B. *Biochim. Biophys. Acta* **1982**, *704*, 52−58.
(3) Bazelyansky, M.; Robey, E.; Kirsch, J. F. *Biochemistry* **1986**, *25*, 125−130.
(4) Sussman, J. L.; Harel, M.; Frolow, F.; Oefner, C.; Goldman, A.; Toker, L.; Silman, I. *Science* **1991**, *253*, 872−879.
(5) Stroud, R. M. *Sci. Am.* **1974**, *213*, 74−88.
(6) Blow, D. M. *Acc. Chem. Res.* **1976**, *9*, 145−152.
(7) Kraut, J. *Annu. Rev. Biochem.* **1977**, *46*, 331−358.
(8) Ordentlich, A.; Barak, D.; Kronman, C.; Flashner, Y.; Leitner, M.; Segall, Y.; Ariel, N.; Cohen, S.; Belan, B.; Shafferman, A. *J. Biol. Chem.* **1993**, *268*, 17083−17095.
(9) Selwood, T.; States, S. R. Feasterand, M. J.; Pryor, A. N.; Quinn, D. *J. Am. Chem. Soc.* **1993**, *115*, 10477−10482.
(10) Harel, M.; Quinn, D. M.; Nair, H. K.; Silman, I.; Sussman, J. L. *J. Am. Chem. Soc.* **1996**, *118*, 2340−2346.
(11) Henderson, R. *J. Mol. Biol.* **1970**, *54*, 341−354.
(12) Marquart, M.; Walter, J.; Deisenhofer, J.; Bode, W.; Huber, R. *Acta Crystallogr., Sect. B* **1983**, *39*, 480−490.
(13) Robertus, J. D.; Kraut, J.; Alden, R. A.; Borktoft, J. J. *Biochemistry* **1972**, *11*, 4293−4303.
(14) Antosiewicz, J.; McCammon, J. A.; Wlodek, S. T.; Gilson, M. K. *Biochemistry* **1995**, *34*, 4211−4219.
(15) Radić, Z.; Pickering, N. A.; Vellom, D. C.; Camp, S.; Taylor, P. *Biochemistry* **1993**, *32*, 12074−12084.
(16) Radić, Z.; Gibney, G.; Kawamoto, S.; MacPhee-Quigley, K.; Bongiorno, C.; Taylor, P. *Biochemistry* **1992**, *31*, 9760−9767.
(17) Quinn, D. M. **1997**, personal communication.
(18) Pullman, A. Binding sites of acetylcholine in the aromatic gorge leading to the active site of acetylcholinesterase. In *Modelling of Biomolecular Structures and Mechanisms*; Pullman, A., Jortner, J., Pullman, B., Eds.; Kluwer Academic Publishers. 1995; pp 11−23.
(19) Gibney, G.; Camp, S.; Dionne, M.; MacPhee-Quigley, K.; Taylor, P. *Proc. Natl. Acad. Sci. U.S.A.* **1990**, *87*, 7546−7550.

S0002-7863(97)00395-8 CCC: $14.00

stabilization of the transition state in the acylation stage of catalysis. In this report we investigate, via theoretical methods, the role of Glu199 in the initial stages of catalysis, shown schematically as

$$E + S \underset{k_{-1}}{\overset{k_1}{\rightleftharpoons}} ES \xrightarrow{k_2} ET \xrightarrow{k_3} EA + P_1 \qquad (1)$$

where transformation of the Michaelis complex *ES* into tetrahedral intermediate *ET* is assumed to be irreversible ($k_3 \gg k_{-2}$), because the pK_a value of a product choline is expected to be smaller than that of catalytic Ser200 due to electron withdrawal effect of the $N(CH_3)_3^+$ group (see, for example, ref 20), implying that acetylation of Ser200 is more favorable than that of choline. In reaction sequence 1 *EA* and P_1 represent acylenzyme and the first product of the hydrolysis, respectively.

First, we used electrostatic and Brownian dynamics simulations to evaluate the effect of the Glu199Gln mutation upon the electrostatic potential inside the active site of AChE and the rate constant of diffusional encounter, k_1, leading to the formation of Michaelis complex between AChE and a positively charged substrate. Then, we used quantum chemical calculations to estimate the effect of the above mutation upon the energetics of the first chemical stage of catalysis, the formation of the tetrahedral adduct between Ser200 and the ester substrate, *ET*, occurring with a rate constant k_2.

Methods

Electrostatic and Brownian Dynamics Simulations. The procedure for estimating the diffusional encounter rate constants for the AChE-ligand system has been described previously.[14] The same procedure was used in the present work, thus only a very brief description of fundamental aspects is provided here.

The steady-state bimolecular rate constant, k_1, for diffusional encounter between an enzyme and its ligand can be represented as[21]

$$k_1 = k(b)\cdot\beta \qquad (2)$$

where $k(b)$ is the rate at which the ligand initially reaches a spherical surface of radius b centered on the enzyme. If b is chosen large enough that the potential of mean force, U, between the reactants is centrosymmetric for distances larger than b, then $k(b)$ can be found by solving the one-dimensional diffusion equation:

$$k(b)^{-1} = \int_b^\infty \frac{e^{U(r)/k_B T}}{4\pi D r^2} \mathrm{d}r \qquad (3)$$

where k_BT is Boltzmann's constant multiplied by temperature, and D is the relative diffusion coefficient. The quantity β is the probability that a ligand started at a random location on the "b (begin) surface" will eventually satisfy appropriate reaction criteria (i.e., diffuse to within a certain distance from the catalytic triad).

The probability β is estimated by generation of a large number of Brownian dynamics trajectories of the ligand around the enzyme and by determining the fraction of trajectories β' resulting in a reactive encounter[22,21]

$$\beta = \beta'[1 - (1 - \beta')\Omega]^{-1} \qquad (4)$$

where Ω is $k(b)/k(q)$ and accounts for trajectories that wander beyond the "q (quit) surface" that might then turn around and react. The trajectories are started with the diffusing substrate on the b surface and are stepped along using the following equation

$$\mathbf{r} = \mathbf{r}_0 + (k_B T)^{-1} D\mathbf{F}(\mathbf{r}_0)\Delta t + \mathbf{R} \qquad (5)$$

where $\boldsymbol{r}_0$ is the position before a step is taken, k_BT and D have the same meaning as in (3), $\boldsymbol{F}(\boldsymbol{r}_0)$ is the force on the substrate at $\boldsymbol{r}_0$, Δt is the timestep, and $\mathbf{R}$ is a stochastic force to account for the random buffeting by the solvent that the diffusing particle would feel if the solvent were represented explicitly.

Calculations were based on the TcAChE crystal structure published by Sussman and co-workers.[4] Electrostatic calculations and Brownian dynamics simulations were performed with the UHBD software.[23,24] Generation of the electrostatic potential map for TcAChE requires prior computation of the average charges of all ionizable residues of the protein. Our approach is based on the assumption that the difference in protonation behavior of a given group in the isolated amino acid and in the protein environment results exclusively from differences in electrostatic interactions in those two environments. The required electrostatic calculations were performed using the finite-difference Poisson−Boltzmann (PB) method,[25] according to a single-site titration site model.[26] For each ionizable site i, ($i = 1, ..., M$), we calculated its free energy of ionization in the otherwise neutral protein, relative to the energy of ionizing this residue when it is free in solution, $\Delta\Delta G_i$. The effective electrostatic interaction energy of this site with other sites with higher indices, $\Psi_{i,j}$,($j = i + 1, ..., M$), where M is the total number of ionizable sites, were also computed. The single-site procedure requires 2 UHBD runs per titratable site to provide all data required for the electrostatic free energy matrix. The corresponding multiple site titration problem is treated in the present work by a Hybrid approach.[27] The energies $\Delta\Delta G_i$ and Ψ_{ij} are used by the Hybrid program to evaluate electrostatic energies of the protein in given protonation states, and based on these energies, equilibrium electrostatic properties are obtained. The resulting average charges of all ionizable residues are used to generate the corresponding electrostatic potential around the enzyme and inside its active site gorge with the finite-difference PB technique. Calculations were done at an ionic strength corresponding to 150 mM of monovalent salt, a temperature of 300 K and at pH 7.

All reaction criteria for the calculation of probability β (eq 1) are shown schematically in Figure 1. Diffusional rate constants reported in the present work are based on 3000 Brownian trajectories for each for the wild-type and mutant enzymes. For all other details see Antosiewicz et al.[14]

Quantum Chemical Calculations. All ab initio calculations were performed with the Gaussian94 program[28] using the standard 3-21G basis set. Two different models of the AChE active site and substrate were used for both the wild-type and the Glu199Gln mutant, as follows:

(20) March, J. *Advanced organic chemistry, reactions, mechanisms, and structure*; John Wiley & Sons: New York, 1992.
(21) Madura, J. D.; Davis, M. E.; Gilson, M. K.; Wade, R. C.; Luty, B. L.; McCammon, J. A. *Rev. Comput. Chem.* **1994**, *5*, 229−267.
(22) McCammon, J. A.; Northrup, S. H.; Allison, S. A. *J. Phys. Chem.* **1986**, *90*, 3901−3905.
(23) Davis, M. E.; Madura, J. D.; Luty, B. A.; McCammon, J. A. *Comput. Phys. Commun.* **1991**, *62*, 187−197.
(24) Madura, J. D.; Briggs, J. M.; Wade, R. C.; Davis, M. E.; Luty, B. A.; Ilin, A.; Antosiewicz, J.; Gilson, M. K.; Bagheri, B.; Scott, L. R.; McCammon, J. A. *Comput. Phys. Commun.* **1995**, *91*, 57−95.
(25) Warwicker, J.; Watson, H. C. *J. Mol. Biol.* **1982**, *157*, 671−679.
(26) Antosiewicz, J.; McCammon, J. A.; Gilson, M. K. *J. Mol. Biol.* **1994**, *238*, 415−436.
(27) Gilson, M. K. *Proteins: Struct. Funct. Gen.* **1993**, *15*, 266−282.

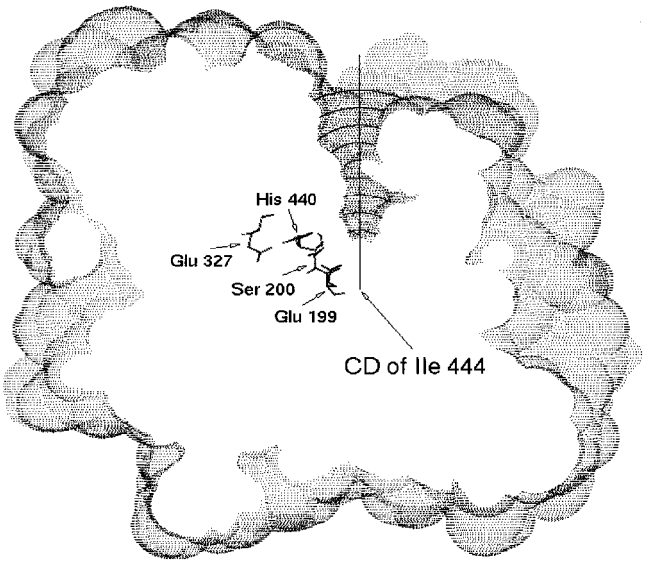

Figure 1. Cross-section of the surface of TcAChE, showing the diffusional encounter surfaces for the AChE ligand system, considered in the present work. Nine surfaces visible in the figure are encounter surfaces along the gorge axis, positioned from 22.7 to 6.7 Å from the C_δ atom of Ile444, every 2 Å. The surfaces monitor attraction of ligands toward the bottom of the active-site gorge. For more details see Antosiewicz et al.[14] This figure was generated with the insightII program and associated modules.[35]

I: Wild-type model, WI, consisted of the side chains of the three catalytic residues (Ser200, His440, Glu327), Glu199 and the substrate, while a model of the mutant, MI, was obtained by physical removal of Glu199 from WI.

II: Model WII contained the same species as WI plus the oxyanion hole which is formed by the backbone amide NH groups of Gly118, Gly119, and Ala201. MII was obtained by replacing Glu199 in WII with Gln199.

The following molecules in their ground electronic states were used to model the various components of the active site: Serine was represented by ethanol, glutamates by butanoate anions, histidine was mimicked by 4-ethylimidazole, glutamine by butanamide, each of the three components of the oxyanion hole by ammonia molecules, and the substrate was selected to be methylacetate. We used this small neutral ester as a substrate rather than ACh^+ in order to reduce computer time. Although, in principle the rate of covalent bond formation between Ser200 and the substrate may depend on the substrate charge, we believe that for ACh^+ the effect of a positive charge located on trimethylammonium group can be neglected at this stage of catalysis, because it is removed by four covalent bonds from the carbonyl carbon atom. In fact, recent mutagenesis experiments on the kinetics of tetrahedral complex formation between mouse AChE and neutral/charged trifluoroketons (TFKs), TFK0 and TFK^+, (TFK0 = *m*-(*tert*-butyl)trifluoroacetophenone; TFK^+ = *m*-(*N*,*N*,*N*-trimethylammonio)trifluoroacetophenone)[29] corroborate our assumption.

Table 1 summarizes the constituents of the models. The only constraint imposed and applied to all of models was fixing of the positions of the four carbon atoms representing the C_α atoms of Glu327, Ser200, His440, Glu199(Gln199) and the three nitrogen atoms representing the peptidic N atoms of Gly118, Gly119, and Ala201, to their positions in the crystal structure.[4] The starting locations of all other non-hydrogen atoms were also set to their crystal structure positions. Mutation to obtain model MII was done by replacing the $O_{\epsilon 2}$ atom in butanoate (model for Glu199) by an amino group. The initial ester substrate position was arbitrarily oriented in such a way that its carbonyl carbon atom was close to the oxygen of ethanol (O_γ atom of Ser200), and its carbonyl oxygen atom in the second set of models (II) could form hydrogen bonds with the ammonia molecules, which represent the oxyanion hole. Our model of the Michaelis complex (*ES* in eq 1) corresponded therefore to the optimized structure of the relevant gas-phase ion−molecule complex under the above mentioned constraints. For example, the WI model is represented in Chart 1, with a total charge of $-2e$.

Table 1. Constituents of the Active-Site Models Used in ab Initio SCF Calculations

model	components	charge
WI	$2CH_3CH_2CH_2COO^-$, $C_2H_5C_3N_2H_3$, CH_3CH_2OH, CH_3COOCH_3	−2
WII	$2CH_3CH_2CH_2COO^-$, $C_2H_5C_3N_2H_3$, CH_3CH_2OH, CH_3COOCH_3, $3NH_3$	−2
MI	$CH_3CH_2CH_2COO^-$, $C_2H_5C_3N_2H_3$, CH_3CH_2OH, CH_3COOCH_3	−1
MII	$CH_3CH_2CH_2COO^-$, $CH_3CH_2CH_2CONH_2$, $C_2H_5C_3N_2H_3$, CH_3CH_2OH, CH_3COOCH_3, $3NH_3$	−1

Chart 1

$$\underset{\text{Glu-327}}{CH_3CH_2CH_2COO^-}\cdot\underset{\text{His-440}}{CH_3CH_2C_3N_2H_3}\cdot\underset{\text{Ser-200}}{CH_3CH_2OH}\cdot$$

$$\underset{\text{Glu-199}}{CH_3CH_2CH_2COO^-}\cdot\underset{\text{substrate}}{CH_3COOCH_3}$$

Formation of the tetrahedral intermediate in the AChE−substrate system was modeled by isomerization of the *ES* complexes such that a covalent bond was formed between the carbonyl carbon of methyl acetate and the oxygen from ethanol with simultaneous proton transfer from ethanol to the nitrogen atom of 4-ethylimidazole. In all cases, the geometries of the substrates corresponding to the Michaelis complexes (*ES* in eq 1), transition states (*TS*), and products representing the tetrahedral intermediates (*ET* in eq 1) were optimized, subject to the constraints mentioned earlier. Additionally, in the case of the two forms of model I, potential energy plots for the isomerization reaction were constructed using the H_γ (Ser200)-$N_{\epsilon 2}$ (His440) distance as the reaction coordinate. It should be stressed here that we use the term transition state (*TS*) to describe the molecular geometry of our model(s) at the top of an energy barrier, having only one negative eigenvalue of the hessian matrix. Also, unless otherwise indicated, the term product refers to the tetrahedral intermediate *ET*, which is the product of the isomerization reaction described by the rate constant k_2 in eq 1.

Due to the relatively small basis set, the lack of the electron correlation effects, and of course the neglect of the rest of the protein, we do not expect our quantum calculations to result in potential energy data which would quantitatively reproduce the experimentally observed kinetic changes upon the Glu199Gln mutation. However, the experimentally observed effect was so large that we hoped they might confirm the hypothesis of the specific role of Glu199 and provide some details on the chemical stage of catalysis.

(28) Frisch, M. J.; Trucks, G. W.; Schlegel, H. B.; Gill, P. M. W.; Johnson, B. G.; Robb, M. A.; Cheeseman, J. R.; Keith, T.; Petersson, G. A.; Montgomery, J. A.; Raghavachari, K.; Al-Laham, M. A.; Zakrzewski, V. G.; Ortiz, J. V.; Foresman, J. B.; Cioslowski, J.; Stefanov, B. B.; Nanayakkara, A.; Challacombe, M.; Peng, C. Y.; Ayala, P. Y.; Chen, W.; Wong, M. W.; Andres, J. L.; Replogle, E. S.; Gomperts, R.; Martin, R. L.; Fox, D. J.; Binkley, J. S.; Defrees, D. J.; Baker, J.; Stewart, J. P.; Head-Gordon, M.; Gonzalez, C.; Pople, J. A. *Gaussian 94, Revision B.1*; Gaussian, Inc.: Pittsburgh, PA, 1995.

Results and Discussion

Electrostatic Properties of Glu199 Mutant. Neutralization of the Glu199 residue has only a small effect on the overall net charge of the enzyme. At pH 7 and an ionic strength of 150 mM, the Glu199 mutant has a charge 0.2 units of elementary charge higher than in the wild-type. This is quite a different behavior than in the case of mutations of surface acidic residues investigated in experimental work by Shafferman et al.[30] and in a recent simulation study by our group,[14] where neutralization of each residue was accompanied by an increase in the net charge of the enzyme by one unit charge. This small effect for the Glu199 mutant results from compensating changes of the average charges of some of the surrounding titratable residues. This phenomenon was discussed previously[31] in connection with the possible presence of positive ion near the catalytic His440 residue in the free enzyme. Briefly, inspection of the average charges of titratable residues for the wild-type and the Glu199 mutant shows that, e.g., at pH 7 and ionic strength 150 mM, in the wild-type, the average charge of Glu199 is −0.81 and the mutation causes a decrease of the average charge of the His440 residue by 0.35 e, and Glu443 by 0.26 e, which leads to the observed 0.2 e increase in the average charge of the whole protein.

Figure 2a shows a comparison between the electrostatic potential along the axis of the active-site gorge of the wild-type and that of the Glu199 mutant. This potential is nearly the same for both enzymes in the region around the entrance to the active-site gorge continuing to some distance inside the gorge. However, from the "choke point" visible in Figure 1, the potentials in both systems begin to differ significantly. In addition, the gradients of the potential along the axis are of opposite sign. This picture is qualitatively different than for the mutants of acidic surface residues.[14]

Active Site−Substrate Encounter Rate. Figure 2b shows the computed diffusional encounter rate constants for different reaction distances, for the wild-type of TcAChE, and for the Glu199Gln mutant. The numerical values with statistical errors are given in Table 2. Comparing those rate constants with the potentials along the axis of the active-site gorge one may see that down to approximately 15 Å above the bottom of the gorge both potentials and rate constants for the wild-type and Glu199 mutant are close to each other. Below the "choke point" significant differences both in reaction rates and potentials between wild-type and the mutant are clearly visible. Close to the bottom of the active-site gorge, where the rate constants are approximately constant for different distances from the bottom of the gorge below the choke point, the rate for wild-type is 2 times larger than that for the mutant. This is much less than the experimentally observed decrease in the hydrolysis rate constant. Assuming that diffusional encounter leads to the formation of the Michaelis complex *ES*, we may conclude that neutralization of the Glu199 residue leads to only about a 50% reduction of rate constant k_1. We did not simulate the change in k_{-1} upon mutation; however, our result of 2-fold reduction of k_1 suggests that k_{-1} must be increased by an even larger factor than 2, in order to account for the significantly increased value of $K_m = (k_{cat} + k_{-1})/k_1$.[19] At this point it is obvious that some other than diffusion factors are responsible for further reduction of the second-order rate constant k_{cat}/K_m for the Glu199Gln mutant. They will be described in the next section.

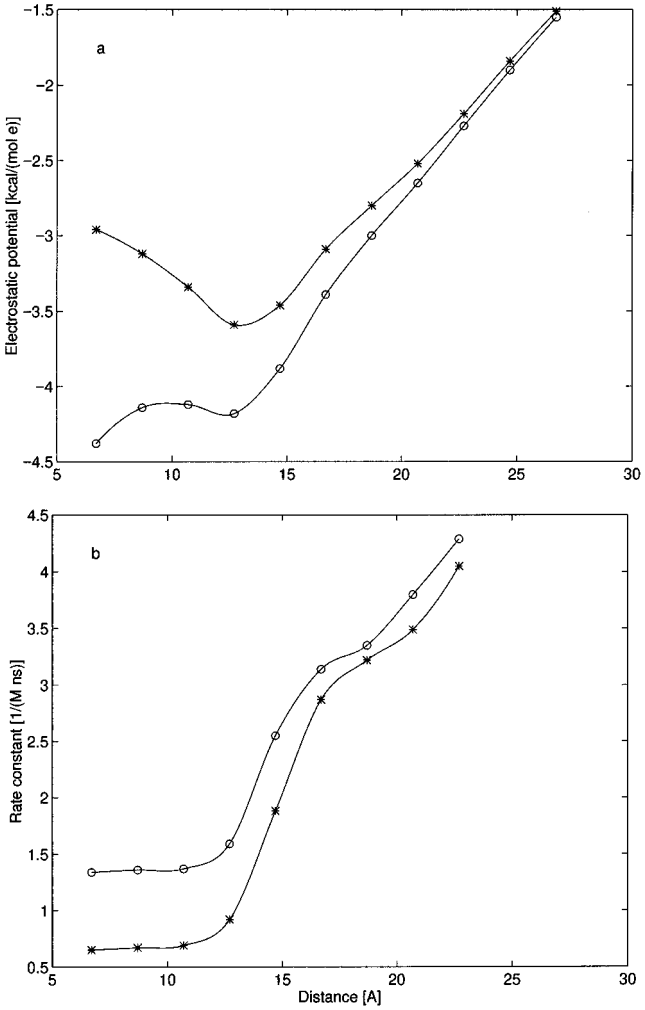

Figure 2. Electrostatic potential, kcal/mol·e (a), and diffusional encounter rate constant k_1, M^{-1} ns^{-1} (b) along the gorge axis. Circles and stars represent the calculated values for the wild-type and Glu199Gln mutant, respectively, while the solid lines are cubic interpolations between them.

Table 2. Computed Encounter Rate Constants, k_1 (in M^{-1} ns^{-1}) for a Cationic Substrate, and the Electrostatic Potential, ϕ (in kcal/mol·e), for Wild-Type TcAChE and the Glu199 Mutant[a]

distance from C_δ of Ile444	wild-type		Glu 199 mutant	
	k_1	ϕ	k_1	ϕ
26.7		−1.51		−1.51
24.7		−1.90		−1.84
22.7	4.29 ± 0.38	−2.27	4.05 ± 0.37	−2.19
20.7	3.80 ± 0.36	−2.65	3.49 ± 0.35	−2.52
18.7	3.35 ± 0.34	−3.00	3.22 ± 0.34	−2.80
16.7	3.14 ± 0.33	−3.39	2.87 ± 0.32	−3.09
14.7	2.55 ± 0.30	−3.88	1.88 ± 0.26	−3.46
12.7	1.59 ± 0.24	−4.18	0.92 ± 0.19	−3.59
10.7	1.37 ± 0.23	−4.12	0.69 ± 0.16	−3.34
8.7	1.36 ± 0.23	−4.14	0.67 ± 0.16	−3.12
6.7	1.34 ± 0.23	−4.38	0.65 ± 0.16	−2.96

[a] Reported values refer to points where the axis of the active-site gorge crosses the surfaces indicated in Figure 1. The distance from the bottom of the gorge is given in Å. The indicated errors bars for the rate constants correspond to 90% confidence limits from the Brownian dynamics simulations.

Tetrahedral Intermediate Formation. In our calculations we assumed that the acylation step of AChE catalysis occurs with the formation of a tetrahedral intermediate as indicated in

(29) Radić, Z. **1997**, personal communication.

(30) Shafferman, A. A.; Ordentlich, A.; Barak, D.; Kronman, C.; Ber, R.; Bino, T.; Ariel, N.; Osman, R.; Velan, B. *EMBO J.* **1995**, *13*, 3448−3455.

(31) Wlodek, S. T.; Antosiewicz, J.; McCammon, A.; Gilson, M. K. Binding of cations and protons in the active site of acetylcholinesterase. In *Modelling of Biomolecular Structures and Mechanisms*; Pullman, A.; Jortner, J., Pullman, B., Eds.; Kluwer Academic Publishers: 1995; pp 25−37.

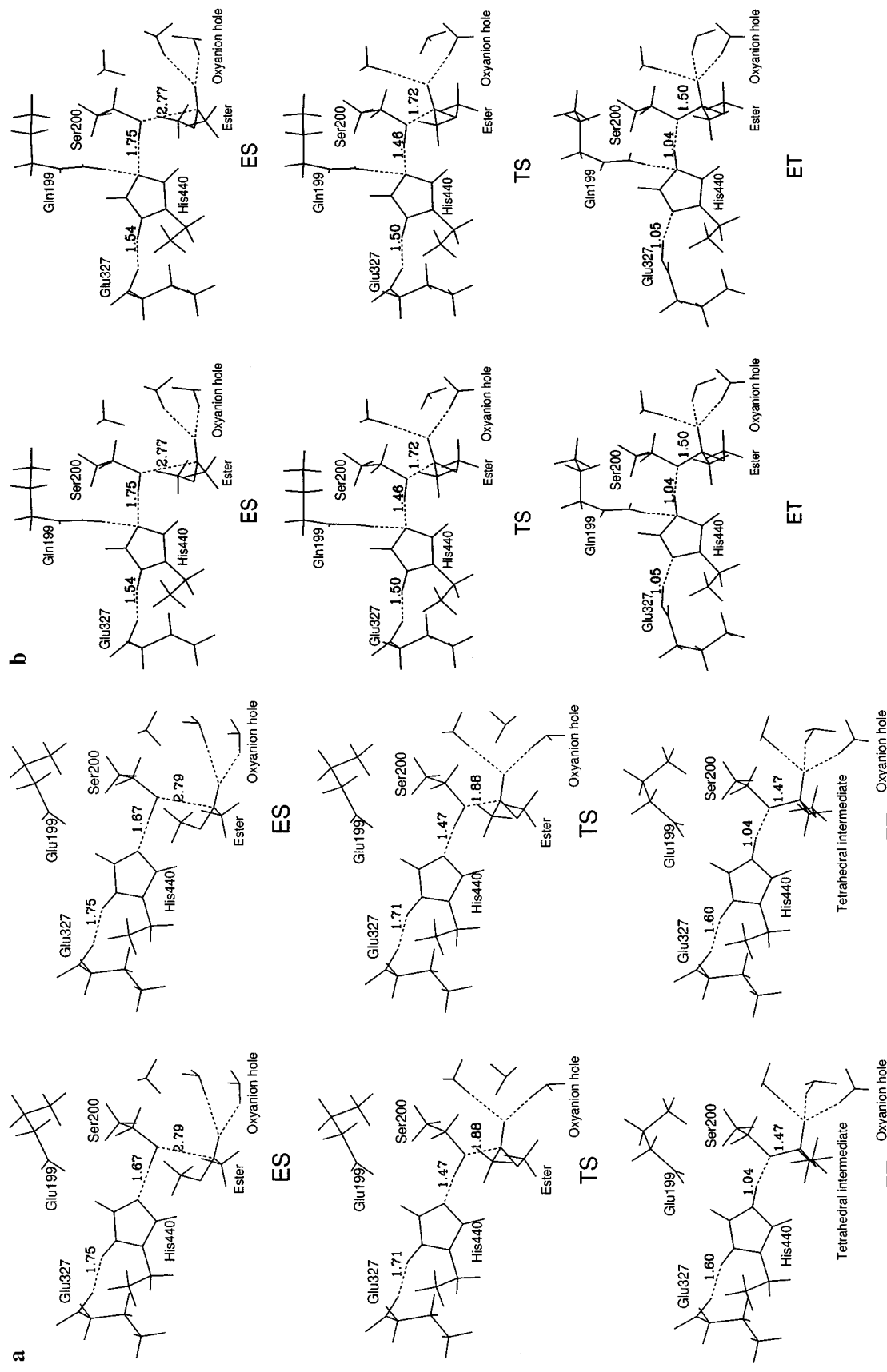

Figure 3. Stereoviews of the ab initio 3-21G structures for the Michaelis complex (*ES*), transition state (*TS*), and product intermediate (*ET*) for the formation of tetrahedral intermediate in model II of the wild-type (a) and the Glu199Gln mutant (b) of the TcAChE-CH_3COOCH_3 model system. Dashed lines indicate hydrogen bonds and the O_δ (Ser200)-$C_{carbonyl}$(CH_3COOCH_3) distance. Interatomic distances are given in Å.

Table 3. Selected Interatomic Distances (in Å) for Three Stationary Points along the Reaction Path in which the Weakly Bound Complex *ES* Is Transformed into a Covalently Bonded Tetrahedral Intermediate *ET* for Two Models of the Wild-Type and Glu199Gln Mutated TcAChE-CH_3COOCH_3 Complex[b]

		distance[a] (Å)				
model	complex	R_1	R_2	R_3	R_4	R_5
	ES	2.77	1.00	1.69	1.02	1.74
WI	TS	1.76	1.16	1.31	1.03	1.69
	ET	1.52	1.53	1.05	1.04	1.63
	ES	2.79	1.01	1.67	1.02	1.75
WII	TS	1.88	1.06	1.47	1.03	1.71
	ET	1.47	1.55	1.04	1.04	1.60
	ES	2.80	1.00	1.71	1.05	1.56
MI	TS	1.79	1.27	1.20	1.07	1.51
	ET	1.57	1.53	1.06	1.08	1.47
	ES	2.77	0.99	1.76	1.05	1.54
MII	TS	1.72	1.06	1.46	1.06	1.50
	ET	1.50	1.54	1.04	1.54	1.05

[a] Distance definitions: R_1: $C_{carbonyl}(CH_3COOCH_3)-O_\gamma$ (Ser200), R_2: O_γ (Ser200)$-H_\gamma$ (Ser200), R_3: $N_{\epsilon 2}$ (His440)$-H_\gamma$ (Ser200), R_4: $N_{\delta 1}$ (His440)$-H_{\delta 1}$ (His440), R_5: $O_{\epsilon 1}$ (Glu327)$-H_{\delta 1}$ (His440). [b] All distances are calculated with the 3-21G basis set.

eq 1. No efforts were undertaken to try to identify the transition state for a possible one-step acylation process similar to that recently suggested by Dive et al.[32]

The structure of the Michaelis complexes (*ES*), transition states (*TS*), and products (*ET*) for the modeled reaction of the formation of the tetrahedral complex in the wild-type and Glu199Gln mutant of TcAChE are shown in Figure 3. The structures refer to our more complete model II. It is evident that the potential energy minimum corresponding to the loose *ES* complexes is characterized by two hydrogen bonds between the carbonyl oxygen of the substrate and two components of the oxyanion hole. It is likely that there are other potential energy minima with respect to the ester orientation in the model *ES* complexes, but we did not attempt to search for them. Rather, we took special care to be sure that this orientation was similar in the wild-type and mutated systems. Two other hydrogen bonds are present in the *ES* complex: one between the hydroxyl group of Ser200 and the $N_{\epsilon 2}$ atom of His440 and the second between the $O_{\epsilon 1}$ atom of Glu327 and $N_{\delta 1}$ of His440. In all cases, as the reaction progressed and the covalent bond was formed between the carbonyl carbon atom of the substrate and the O_γ oxygen atom of Ser200, protons from those hydrogen bonds moved toward their acceptors. This leads to a complete proton transfer from Ser200 to His440 in both systems and from His440 to Glu327 in the case of the mutated system, while in the case of the wild-type only to a shortening of the corresponding hydrogen bond. In other words, our model formally describes a classical general base mechanism for the wild-type enzyme and a charge relay mechanism[33] for the mutated enzyme. The occurrence of the second proton transfer (from His440 to Glu327) is accompanied by a change in conformation of the Glu327 side chain, which apparently changes the orientation of the Glu327 carboxylic group so it can accept the proton from the imidazole ring. Although the occurrence of the His440-Glu327 proton transfer is obviously favored when stabilization of the positive charge on His440 is removed by neutralization of negative charge at position 199, it is possible that it might be an artifact related to the incompleteness of our model (the neglect of other residues of the protein matrix) and to the

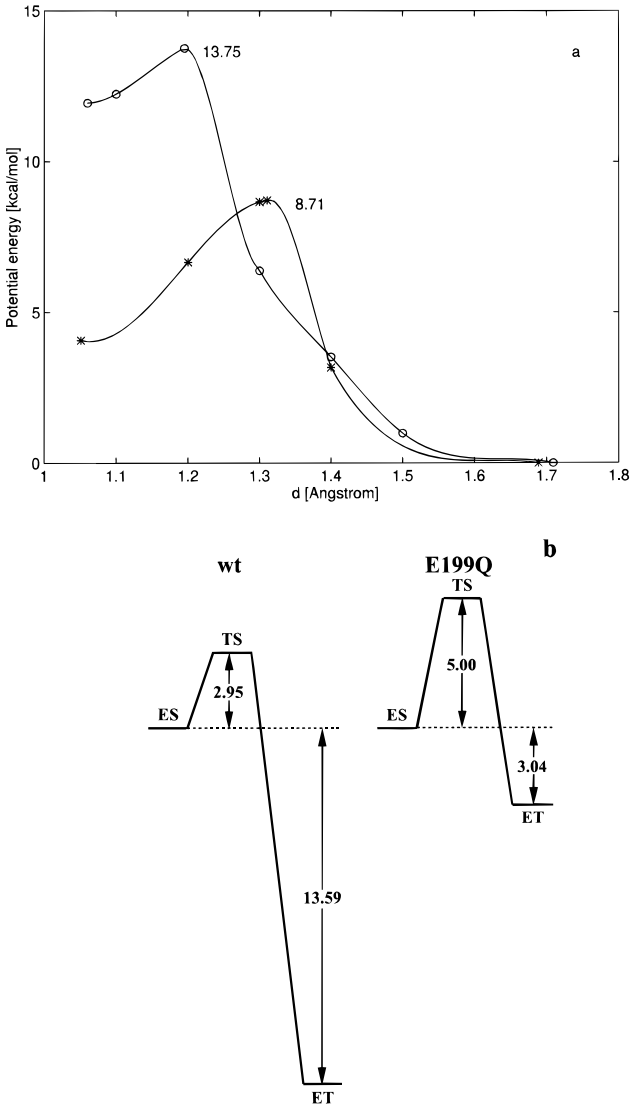

Figure 4. (a) Calculated potential energy profiles for the formation of the tetrahedral intermediate in model WI (stars) and MI (circles). Distance *d* is the interatomic distance between H_γ (Ser200) and $N_{\epsilon 2}$ (His440), in Å. The points at the extreme distances correspond to the *ES* and *ET* complexes, while the maxima represent transition states (*TS*). Solid lines are cubic spline fits to the calculated values. Included numbers indicate the potential barrier heights. (b) Potential energy diagrams for the same reaction calculated with model WII (on the left) and MII (on the right).

incompleteness of the basis set which can overestimate the basicity of butanoate and/or underestimate the acidity of the protonated ethylimidazole in the MII model complexes. On the other hand, we did not observe that kind of behavior in model I. This suggests a possibility that the improved model MII describes the real process in the case of the Glu199Gln mutant. It seems, therefore, that the improved model and the usage of higher quality basis set in future studies and precise proton inventory inhibition experiments can confirm or reject the charge relay mechanism in Glu199Gln AChE.

The critical interatomic distances for all models are gathered in Table 3. It is worth mentioning that all attempts to locate the product complex (*ET*) when Glu327 was absent from the model WI failed, which emphasizes the crucial role of that residue as a member of catalytic triad. Structural data from Table 3 and potential energy data from Figure 4 also point to an important role of the oxyanion hole which facilitates the formation of the tetrahedral intermediate by stabilizing the negative charge of the anionic tetrahedral intermediate. It is

(32) Dive, G.; Dehareng, D.; Peeters, D. *J. Quant. Chem.* **1996**, *58*, 85−107.

(33) Blow, D. M.; Birktoft, J. J.; Hartley, B. S. *Nature* **1969**, *221*, 337−340.

seen, for example, that the transition state *TS* is formed at about 0.1 Å longer distance between the O_γ atom of Ser200 and the carbonyl carbon atom of the substrate (parameter R_1 in Table 3) in the case when the oxyanion hole was included (model WII). Stabilization of the tetrahedral intermediate by the oxyanion hole in AChE was demonstrated also in the hybrid PM3/MM calculations by Vasilyev.[34]

Figure 4 shows the potential energy data for the simulated reactions. It is evident that both models predict a dramatic increase in the reaction potential barrier for the mutant. In fact, a large stabilization of the transition state due to the interaction with the negatively charged Glu199 is postulated by Quinn et al.[17] Here we provide some insight into that stabilization as resulting from attraction between the positively charged imidazole ring of the ionized His440 and the negative charge of carboxyl group of the ionized Glu199. As the reaction proceeds leading to a complete proton transfer from Ser200 to His440, likewise the stabilization increases, leading to significant exothermicity of formation of the tetrahedral intermediate in the wild-type enzyme. Although, in the mutated enzyme, our model MII predicts a hydrogen-bond formation between the NH_2 group of Gln199 and one of the nitrogen atoms of the imidazole ring (Figure 3b). Apparently this interaction is not large enough to compensate for negative charge deletion at position 199. Assuming that entropy effects in the formation of the transition states for the wild-type and Glu199Gln enzymes are similar, while neglecting the possible differences in transmission coefficients, the estimated decrease in the rate constant k_2 at room temperature, based on the energy barrier heights from Figure 4b, is about a factor of 31.9.

Comparison with the Experimental Rate Data. If k_2 describes the slowest stage of catalysis ($k_{cat} = k_2$), its 32-fold reduction upon the Glu199Gln mutation is in reasonable qualitative agreement with the experimentally observed factor of 10 drop of the k_{cat}.[17] The effect on second-order rate contant which from a steady-state approximation for reaction sequence 1 is

$$\frac{k_{cat}}{K_m} = \frac{k_1 k_2}{k_{-1} + k_2} \tag{6}$$

cannot be precisely estimated due to the uncertainty of the ($k_{-1} + k_2$) function behavior. However ($k_{-1} + k_2$) must change much slower that the nominator of (6), so the overall calculated decrease of a factor of 64 for k_1k_2 corresponds well to the experimentally observed drop in k_{cat}/K_m of 50−100 times when Glu199 is neutralized.[16,17]

Conclusions

Calculations described in this study confirm previous findings derived from experiments that a single negatively charged residue at position 199 located in the direct vicinity of the AChE catalytic triad contributes significantly to the catalytic efficiency of the enzyme. Its action has a dual character. First, it significantly lowers the electrostatic potential and generates a favorable gradient at the deepest part of the reaction gorge which enhances diffusional penetration of the positively charged substrate to the reactive site of AChE. Second, it provides substantial stabilization of the transition state for the first chemical stage of catalysis in which a covalent bond is formed between catalytic serine and the substrate. This latter role occurs through the electrostatic interaction with the imidazole ring of the catalytic histidine which becomes protonated upon generation of the tetrahedral intermediate. Our calculations also show a critical role for the oxyanion hole which stabilizes the negative charge of the oxygen atom in the tetrahedral intermediate by making the formation of the intermediate thermodynamically favorable. Finally, our calculations suggest that a charge relay mechanism might be involved in the mutated TcAChE where the negative charge of Glu199 is neutralized. This last conclusion has to be verified, however, in future experimental and theoretical studies.

Acknowledgment. The authors are grateful to Prof. J. A. McCammon, Department of Chemistry & Biochemistry, and Pharmacology, University of California, San Diego, for guidance and support. Gratitude is also expressed to Molecular Simulations, Inc., San Diego, CA for generously providing us with the insightII and Quanta software. J.B. was supported in part by NSF Grant MCB-9596046 to UCSD. J.A. acknowledges support from the Polish State Committee for for Scientific Research (8 T 11 F 00609). A portion of the calculations were performed at the ICM, Warsaw University, Poland. The authors also gratefully acknowledge Dr. Zoran Radić for careful reading of the manuscript and helpful comments and to Dr. Daniel Quinn for discussions and helpful insights.

JA970395V

(34) Vasilyev, V. V. *J. Mol. Str.* **1994**, *304*, 129−141.
(35) MSI. *InsightII*; Molecular Simulations, Inc.: San Diego, CA, 1996.